WALAILAK JOURNAL
http://wjst.wu.ac.th Engineering and Physical Sciences

Accelerated FEM Analysis for Critical Engine Components

Leonardo FRIZZIERO[*] and Luca PIANCASTELLI

Department of Industrial Engineering, Alma Mater Studiorum, University of Bologna, Bologna, Italy

([*]Corresponding author; e-mail: leonardo.frizziero@unibo.it)

Received: 9 January 2014, Revised: 21 April 2014, Accepted: 22 May 2014

Abstract

This paper introduces a method to simplify a nonlinear problem in order to use linear finite element analysis. This approach improves calculation time by 2 orders of magnitude. It is then possible to optimize the geometry of the components even without supercomputers. In this paper the method is applied to a very critical component: the aluminium alloy piston of a modern common rail diesel engine. The method consists in the subdivision of the component, in this case the piston, in several volumes, that have approximately a constant temperature. These volumes are then assembled through congruence constraints. To each volume a proper material is then assigned. It is assumed that material behaviour depends on average temperature, load magnitude and load gradient. This assumption is valid since temperatures vary slowly when compared to pressure (load). In fact pressures propagate with the speed of sound. The method is validated by direct comparison with nonlinear simulation of the same component, the piston, taken as an example. In general, experimental tests have confirmed the cost-effectiveness of this approach.

Keywords: Optimization, simulation, CAD, geometry, FEA

Introduction

State of the art and the new proposal

Nonlinear simulation of piston engines is not as simple as may be expected. Even with the most sophisticated FEA software, it is not rare that true performance are grossly underestimated. For example in an "old" 8 valves common rail piston engine, the limit was fixed by the manufacturer to be around 140 bar. During tests no problem arose up to 160 bar and in many cases 180 bar were reached without problems. Also temperature seems to be out of range, with critical values easily overcome. This fact is due to the fact that the peak pressure and temperatures are reached in very short time and the duration is also very short. The velocity factor could not be ignored in piston FEA.

Even with the proper data, simulation takes a long time. Very nonlinear analysis should be performed with complicated material tables that should take into account temperature, velocity, stress and strain. Convergence is then more difficult than usual and in many cases progressive analysis is required with steps introduced manually into the CAD/FEA model. This process is very time-consuming and leads to errors.

Geometry optimization is beyond possibility and standard geometries are adapted to the many geometrical constraints already present. At first glance it is possible to identify the different "schools" followed by the different manufacturers. Very different geometries are adopted to solve the same problem. This fact may mean that the optimization level is not very high. For this reason a new approach is introduced in this paper. At first a FEA pure thermo dynamical analysis is carried out to individuate maximum temperature values and distribution. Then this continuous temperature 3D map is sampled into a discrete number of values, typically with 5 levels at most. This process permits to isolate volumes with the same temperature level. Then these volumes of the piston with equal temperature level are isolated as

single 3D parts. Then the piston is reassembled to the original shape by using these 3D parts. The FEA analysis is performed by assuming that these parts have perfect adherence (continuity of displacements on the common surface boundaries). By giving the proper tangential elastic modulus to each part it is possible to perform linear analysis instead of highly nonlinear. This is due to the fact that large displacements cannot be present in a piston, in order to preserve the functionality of the piston. The tangential elastic modulus depends on the temperature (obtained by the FEA thermo dynamical simulation) and on the pressure and pressure gradient (usually obtained by a 1D Gas dynamics simulation model of the engine). The linear simulation of this piston assembly with linear material models usually takes seconds on a personal computer. The highly nonlinear traditional method takes hours or days on a supercomputer with the strong possibility that convergence does not take place. In the following example [1-4].

Material properties of the critical component

A good knowledge of the material properties is fundamental for any simulation. In this case the piston is made of the well known aluminium alloy 390-T5. This alloy is commonly used in high performance turbocharged diesel engines. The 390-T5 chemical and mechanical properties are summarized in **Tables 1** and **2** and **Figures 1** and **2**.

Table 1 A390 data.

Chemical composition	
Component	**Weight %**
Al	78
Cu	4 - 5
Fe	Max 1.3
Mg	0.45 - 0.65
Mn	16 - 18
Ti	Max 0.2
Zn	Max 0.1

Table 2 A390 properties.

Mechanical and physical properties		
Hardness	125	HB
Ultimate tensile stress	295	MPa
Yield tensile stress	260	MPa
Young modulus	81.35	°C
Melting temperature	648.88	°C
Specific thermal capacity	0.962	kJ/kg °C
Density	0.0157	kg/m^3

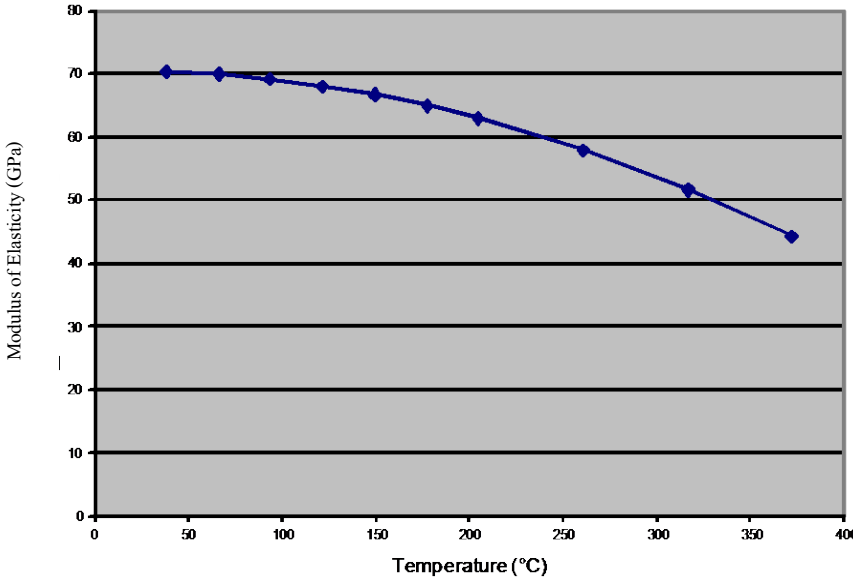

Figure 1 The static modulus of elasticity as a function of temperature.

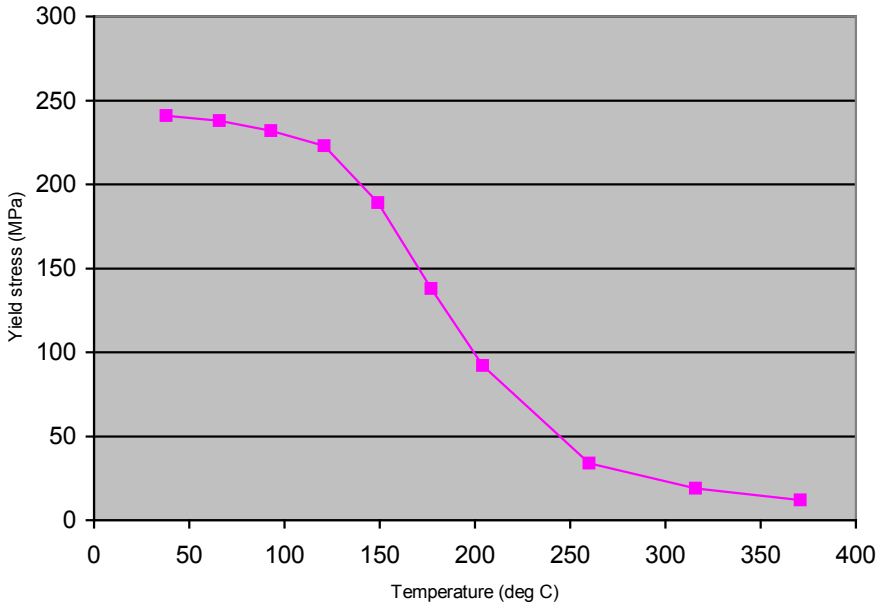

Figure 2 The static yield stress as a function of the temperature.

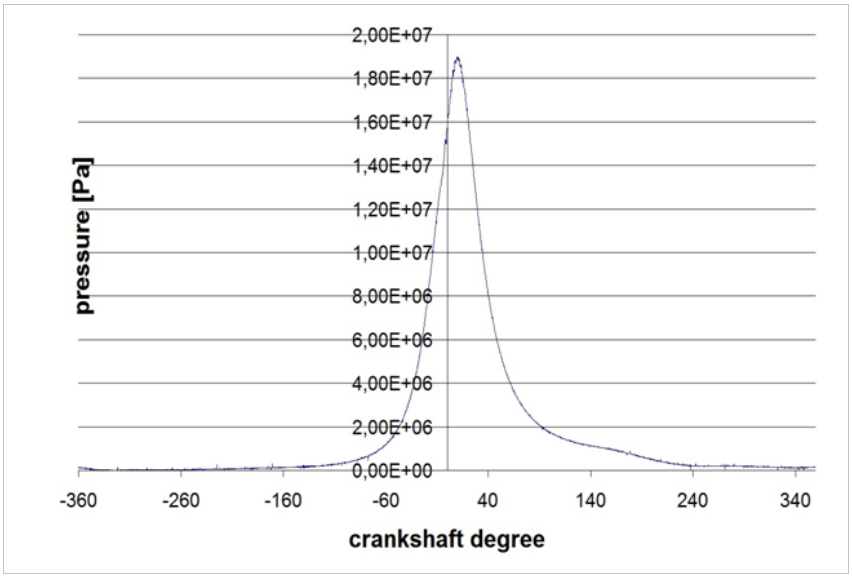

Figure 3 Indicator diagram.

Material properties and velocity of application of loads

Loads are applied on the piston at very high velocity and acceleration (**Figure 3**). Under these condition, both the Young's Modulus and ultimate tensile stress are sensibly higher than quasi-static values. In particular Yield stress tends to approach ultimate tensile stress and the material tends to lose its ductility. Stress to velocity data are very difficult to obtain.

Since pressure gradients are very steep, with values that may easily be up to 1.3×10^8 (bar/s), the increment of pressure inside the cylinder is extremely fast. The crystals that constitute the material do not have the time to modify their properties and the dynamic modulus of elasticity is incremented nearly up to the values of room temperature. For this particular alloy this relationship is kept up to 550 °C. Practically, a hardening process takes places inside the material that deforms plastically, keeping the mechanical properties typical of much lower temperatures. The law of plastic flux is the following (1);

$$\sigma = C\,(d\varepsilon/dt)^m \quad (1)$$

where σ [psi] is the stress and ε is the deformation [-], while C and m are material constants. C and m for the Aluminum alloy 390.0-T5 are summarized in **Table 3**.

Table 3 Aluminum alloy 390.0 T5 material constants.

Temperature (°C)	C (ksi)	m [-]
200	11,6	0,066
400	4,4	0,115
500	2,1	0,211

Table 3 shows that m increases 4 fold as the temperature is varied from 200 to 500 °C, so as the temperature is raised the stress associated to the same strain rate increases 4 folds. So as the temperature increases the influence of the deformation rate on the maximum allowable stress increases. This means that the reaction delay to the load (or inertia) of the material increases with the temperature. The higher the deformation rate the lower the stress felt by the material for instantaneous loads. This fact is truer as the temperature rises. **Table 4** gives the true elastic modulus with a pressure gradient of 1.3×108 (bar/s). With this stress rate, the influence of temperature is limited to 70,000/48,000 = 1.48 for the tangential Elastic Modulus and 135/65 = 2 for the Yield Stress. With static loads the elastic modulus reduction would have been the same (**Figure 1**) while the Yield Stress reduction is more than 248/2 = 124 (**Figure 2**). Practically the material doesn't resist to any static stress over 350 °C. On the contrary, at high stress rate and for an extremely short time, the material is still resistant up to 500 °C. This is due to the material inertia. This is the reason why models based on a liquid behavior instead of a solid one are used for explosive and bullet impact simulations.

Table 4 A390 T5 alloy material properties with a combustion chamber pressure gradient of 1.3×10^8 [bar/s], the data were extrapolated from experimental data from forging of parts of the same material and simulations with explicit FEA code.

Temperature (°C)	Modulus of elasticity (MPa)	Yield stress (MPa)	Ultimate stress (MPa)
497	48,000	65	80
483	48,000	63	82
412	60,000	70	100
330	62,000	75	105
314	68,000	80	110
292	68,000	82	110
263	68,000	130	200
256	68,000	130	200
233	70,000	130	200
208	70,000	135	208

The FEA with the proposed linearized model

In our case the analysis starts from experimental data with lower-than-required thermal loads and power output (**Figure 4**). This makes it possible to tune the thermodynamic simulation model and to upgrade it to the required power level [5-7].

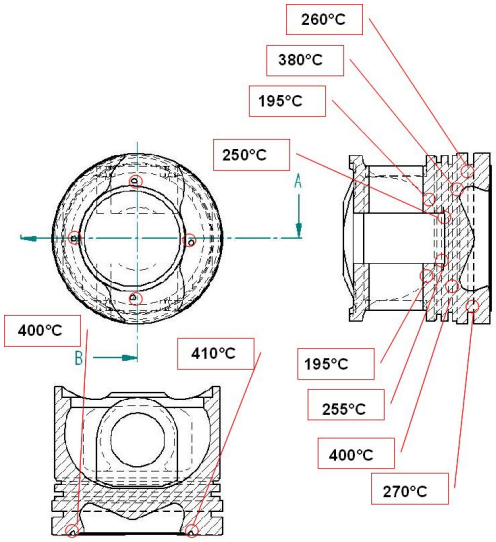

Figure 4 Illustration of the experimental temperature measured on the piston with an original thermal load.

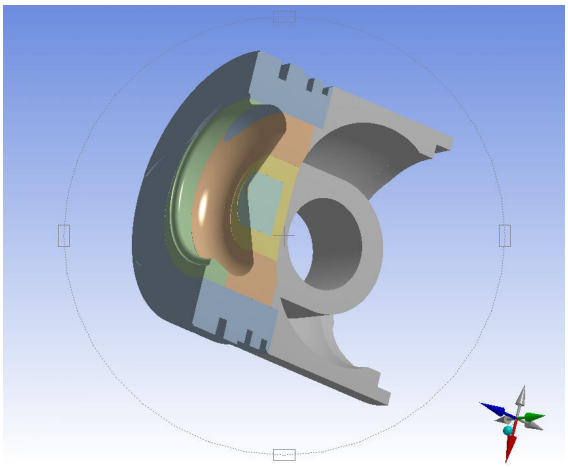

Figure 5 Different volumes with different peak temperatures (green = 487 °C, blue = 483 °C, brown = 333 °C, yellow = 383 °C, greyblue = 412 °C (center combustion chamber), blue = 283 °C, grey = 213 °C) (Colors are available in online format).

In **Figure 5** the different volumes for the different temperature peak level are depicted. The software considers these zones as perfectly adherent, so congruence of displacements is automatically imposed on boundary surfaces [8-12].

Computing

Linear FEA mesh [13-16]

Figure 6 shows the FEA mesh with the due refinement. The software takes the assembly as is and it "creates" a mesh. Due refinement is then added on fillet and geometrically complicated points.

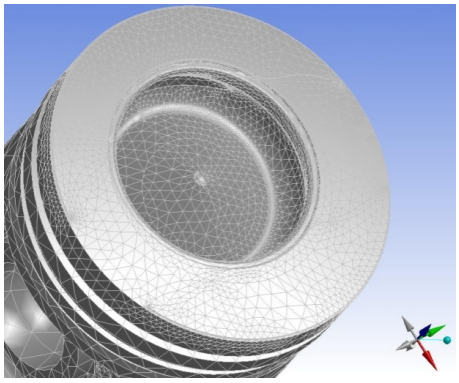

Figure 6 Mesh for linear solution.

Constraints

The piston should slide in the cylinder and for this purpose it has been considered the constraint through the rings. The piston can also freely rotate around the piston pin. **Figures 7** and **8** show the constraints on FE model.

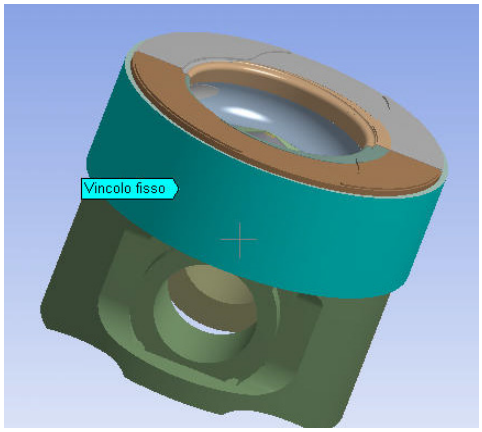

Figure 7 Ring constraints that simulate the cylinder wall (green). "vincolo fisso" means "fixed constraint" and is applied to the external surface of the ring (Colors are available in online format).

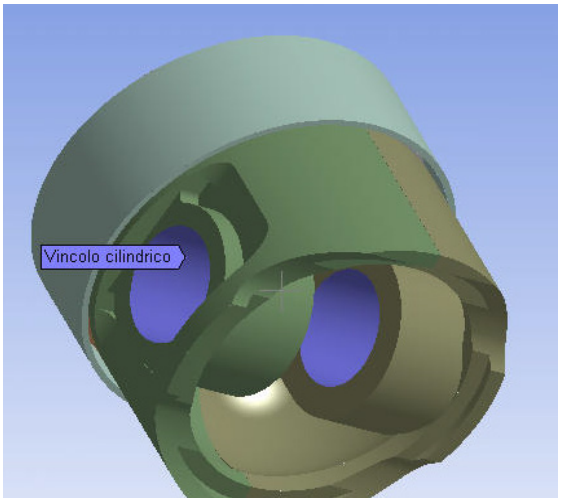

Figure 8 Cylindrical constraints that simulate the pin. "Vincolo cilindrico" means bearing constraint and is applied to the 2 cylindrical surfaces (blue color) where the pins works (Colors are available in online format).

Loads

The total load that affects the piston is composed of the pressure and thermal load. The thermal load is already embedded in the model through volumes with different material properties, so only the pressure loads need to be applied. The pressure load is simulated by the application of different pressure on different piston top surfaces. The different pressure values have been evaluated through the simplified method of Piancastelli [17-21]. Average values of 160 bar inside the combustion chamber and of 140 bar on the remaining piston surface have been applied on the FEA model both for the nonlinear and linear analysis.

Results of the simplified analysis

Figures 9 and **10** show stress fields and safety factors from the FEA simulation. The piston was loaded with a pressure of 180 bar in the combustion chamber and of 160 bar on the piston top.

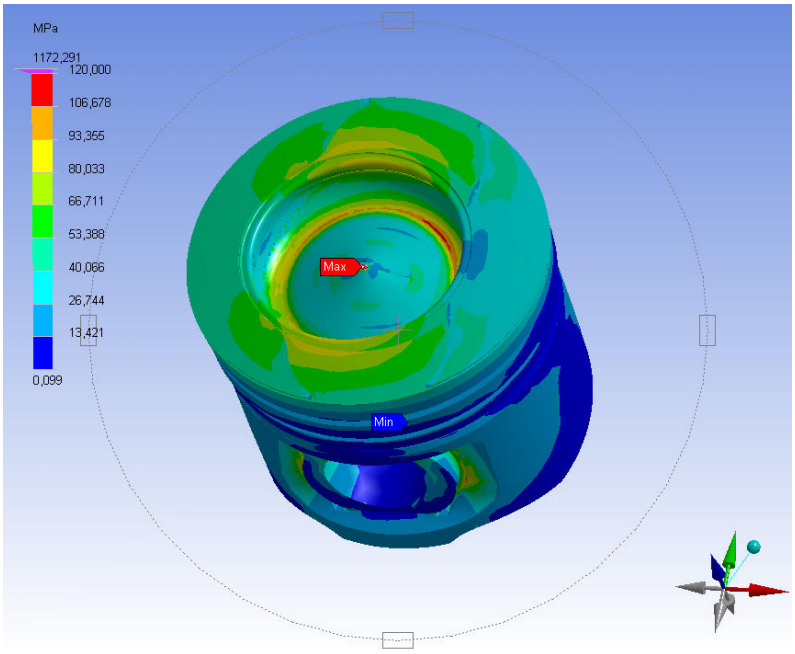

Figure 9 Pressure stresses at 160 - 180 bar from 120 MPa (red) down to 13.4 MPa (dark blue). The maximum value of 1172 MPa is not depicted in this figure and depends on the boundary condition on a coarsely modeled sharp edge (Colors are available in online format).

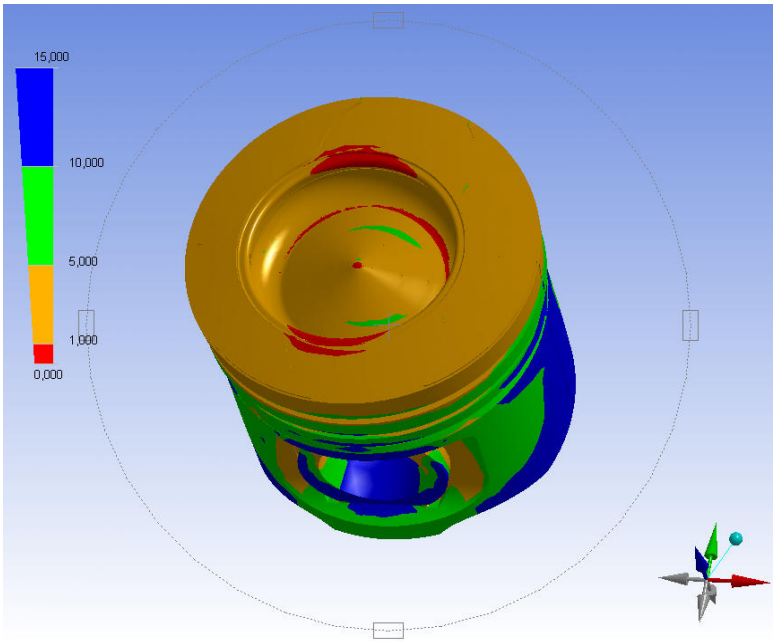

Figure 10 Safety factor at 160 - 180 bar from 15 (dark blue) down to values of 1.00 (red). The original piston is not verified at this pressure level (Colors are available in online format).

In **Figure 10** it can be seen that the piston does not resist in the internal fillet of the combustion chamber. In fact the red color indicates that the material safety factor is less than 1. The safety factor is calculated as the ratio between the calculated stress and the yield stress. The only feasible solution is to change piston geometry, by increasing the fillet or by expanding the combustion chamber inside the piston. A flatter and less profound combustion chamber is a first solution, another possible solution is to improve piston cooling through a duct inside the piston. The larger fillet solution is adopted in **Figure 11**. This solution makes it possible to increase significantly the safety factor up to a minimum value of 2.

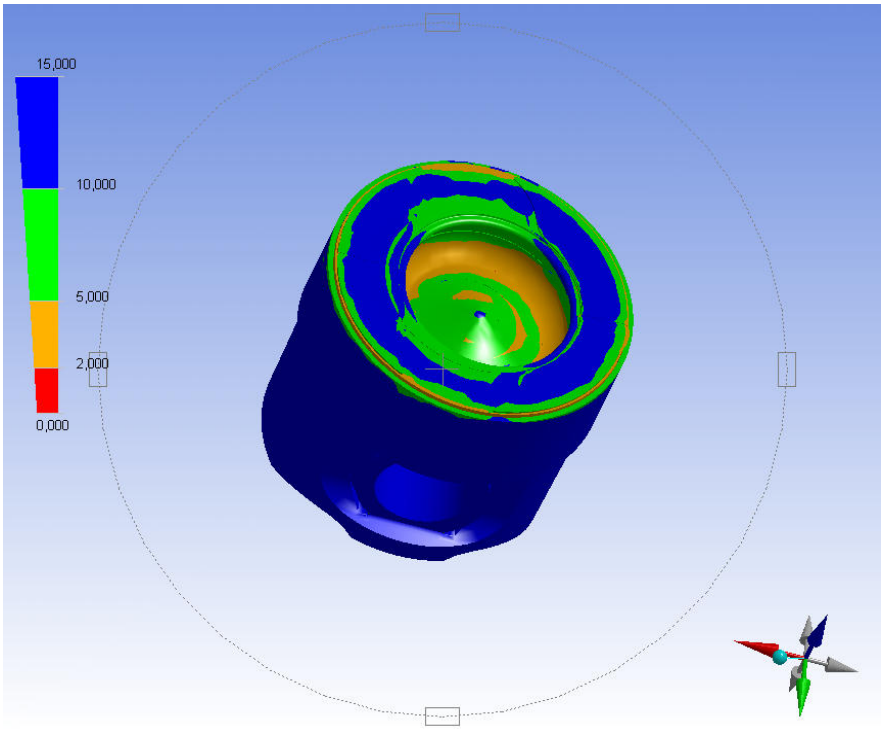

Figure 11 New geometry with pressure 140 (outside the combustion chamber) - 160 bar (inside the combustion chamber). No red color is present and the safety factor is above 2 everywhere (Colors are available in online format).

Nonlinear FEA mesh

A traditional nonlinear model has been implemented in order to compare the simplified linear approach with the traditional nonlinear solution. In order to make it possible to obtain a solution in a reasonable time only the half of the piston has been considered. For this purpose we have been used 10-nodes tetrahedral elements. The constraints and the loads are the same of the previous linearized model. **Figure 12** shows the nonlinear mesh.

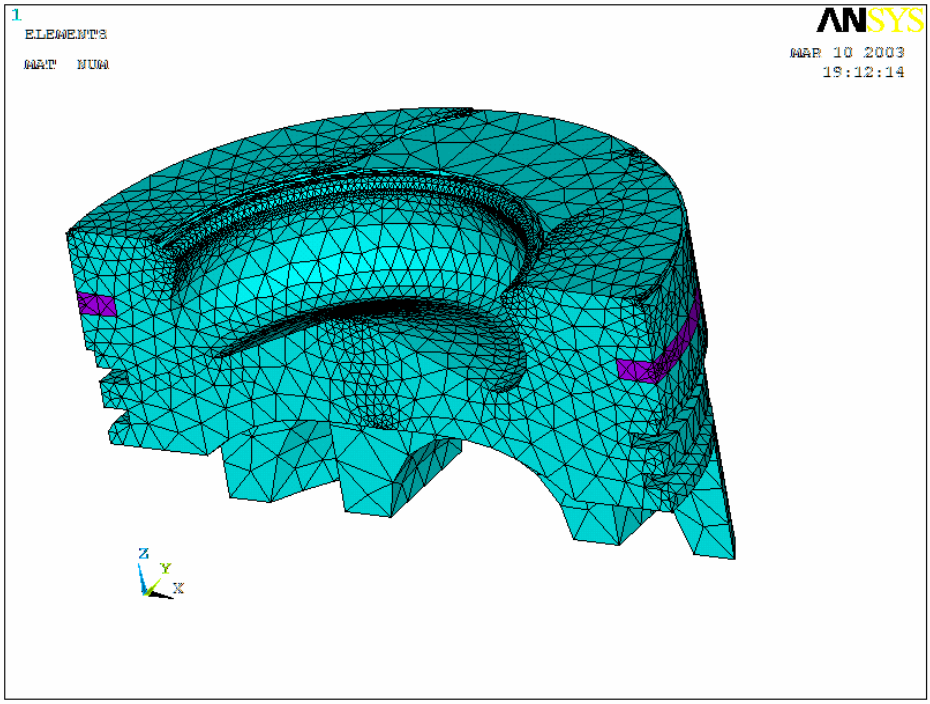

Figure 12 Nonlinear mesh.

Non liner analysis
The thermal flow value and the faces (walls) exchange coefficients were considered as follows:

- Adiabatic faces (walls) of the piston.
- Thermal flow consequently found.
- Material characteristics, constraint system and thermal and structural loads as above.

Figures 12 - 14 show the thermal and pressure loads and the boundary conditions.

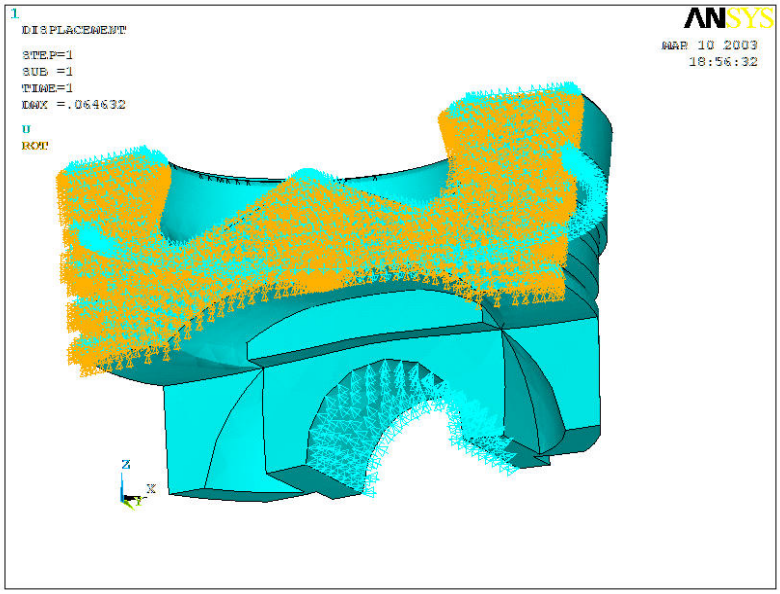

Figure 12 Constraints, only half of the piston was simulated. Even with this simplification, 2 whole days of computer time were necessary.

It has been necessary to impose the symmetrical constraint in order to analyze only half of the piston (yellow arrows in **Figure 12**). Cylindrical constraints were also added in the piston-pin contact area. A radial boundary condition was added to simulate piston rings.

The temperature application field goes from a maximum of 490 °C on the top (red) to 208 °C (green) at the bottom of the piston, as it can be seen in **Figure 13**. No blue values are present on the piston in the results.

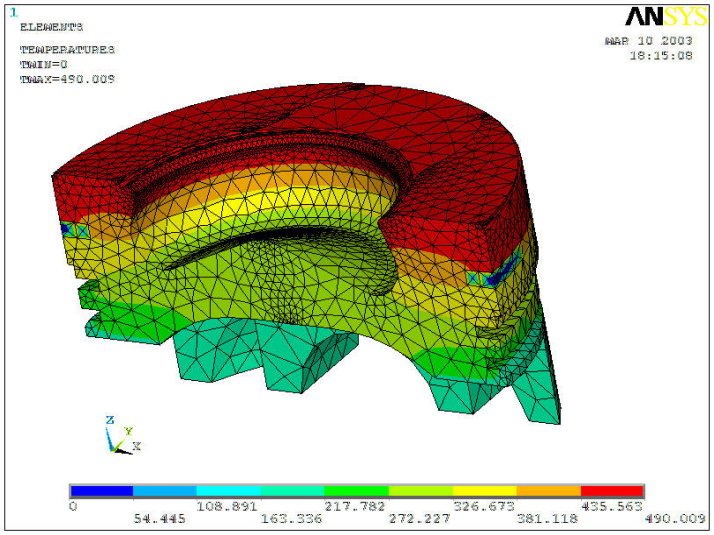

Figure 13 Temperature distribution (Colors are available in online format).

The results depicted in **Figure 14** show that the original piston cannot bear a maximum pressure of 160 bar, the combustion chamber fillet (red) is again the critical point [22-25]. This is the same result as the linearized model proposed. This calculation took 2 days of computer time on our best computer (a 256 GB RAM PC), while the linearized simplified method proposed in this paper took less than 5 min on a very common laptop.

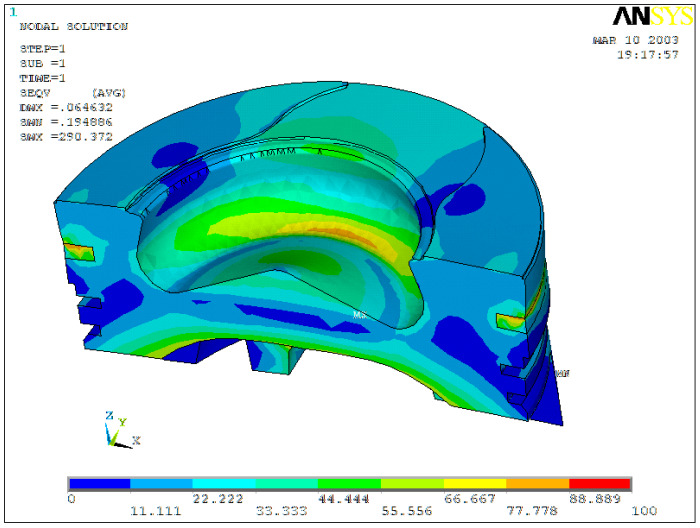

Figure 14 Nonlinear FEA results on the original piston with a peak pressure of 180 bar and a chamber pressure on piston top of 160 bar (Colors are available in online format) [26-30].

Conclusions

The linearized analysis gives the same results even on a very "difficult" component like an aluminium-alloy-diesel-direct-injection piston. This validates the method at least for aluminum alloy components, similar analyses have been performed on high temperatures alloys with even better accordance between linearized and nonlinear analysis. The components have then been tested on the engines with increased performance. No experimental data were collected on the upgraded parts with the new higher power level. However, the new parts run without problems.

The linearized method, with its much reduced convergence time, makes it possible to optimize the components, operation that is not feasible with nonlinear analysis even with modern supercomputers. This is due to the fact that the linearized method always converges to a solution in a very limited computer time (< 5 min on a laptop), while the same piston with a standard nonlinear model took 2 days of computer time (> 48 h) on our very best PC. It is fortunate that the model converged after this time. This fact is uncommon and manual steps are usually performed to reach convergence. The results of the proposed linearized method and the nonlinear model are very similar. The maximum stress for the nonlinear analysis is 100 MPa (**Figure 14**), while the linearized method gave 106 MPa (**Figure 9**). The point of maximum stress is very close. The maximum value in the center of the combustion chamber of the linearized model (about 120 MPa) should not be considered since it is due to distorted FE elements (**Figure 9**).

References

[1] D Kuchemann and J Weber. *Aerodynamics of Propulsion*. Mc Graw-Hill, 1953.
[2] WM Kays and AL London. *Compact Heat Exchanger*. Mc Graw-Hill, 1955.
[3] SF Hoerner. *Fluid Dynamic Drag*. Hoerner, 1965.
[4] B Gothert. *The Drag of Airplane Radiators with Special References to Air Heating*. NACA report n°896, 1939.
[5] H Winter. *Contribution to the Theory of the Heated Duct Radiator*. NACA report n°893, 1939.
[6] FW Meredith. *Note on the Cooling of Aircraft Engines with Special References to Ethylene Glycol Radiators Enclosed in Ducts*. British A.R.C. memorandum n°1683, 1935.
[7] A Weise. *The Conversion of Energy in a Radiator*. NACA report n°869, 1938.
[8] WJ Nelson, KR Czarnecki and RD Harrington. *Full-Scale Wind-Tunnel Investigation of Forward Underslung Cooling-Air Ducts*. NACA report n°L115, 1944.
[9] KR Czarnecki and WJ Nelson. *Wind-Tunnel Investigation of Rear Underslung Fuselage Ducts*. NACA report n°L438, 1943.
[10] Ames Research Staff, Equations. *Tables and Charts for Compressible Flow*. NACA report n°1135, 1953.
[11] JF Johnston. *Review of Flight Tests of NACA C and D Cowlings on the XP-42 Airplane*. NACA report n°771, 1943.
[12] C McLemore. *Wind Tunnel Tests of a 1/20-Scale Airship Model with Stern Propellers*. NASA-TN-1026, Technical Note, Langley Research Center, 1962.
[13] AI AA-26-2693. *Aerodynamic design of Low Speed Aircraft with a NASA fuselage Wake/Propeller Configuration*. Dayton Ohio, 1986.
[14] JT Lowry. *The Bootstrap Approach to Aircraft Performance*. Part Two, Constant-Speed Propeller Airplanes, 1999.
[15] Spinning the Fuselage to Save Fuel, Available at: http://www.flightglobal.com/.../russian-tsagi-spinning-the-fuselage-to-save-fuel, accessed September 2011.
[16] L Piancastelli and M Pellegrini. The bonus of aircraft piston engines, and update on the Meredith effect. *Int. J. Heat Tech.* 2007; **25**, 51-6.
[17] J Kurzke. *Achieving Maximum Thermal Efficiency with the Simple Gas Turbine Cycle*. MTU Aero Engines, Dachauer Str. 665, 80995 München, Germany.
[18] RC Wilcock, JB Young and JH Horlock. *Gas Properties as a Limit to Gas Turbine Performance*. ASME GT-2002-30517, 2002.
[19] L Piancastelli, G Caligiana, F Leonardo and S Marcoppido. Piston engine cooling: an evergreen problem. *In*: Proceeding of the 3rd CEAS Air & Space Conference, Venice, Italy, 2011.
[20] L Piancastelli, L Frizziero, E Morganti and A Canaparo. Fuzzy control system for aircraft diesel engines. *Int. J. Heat Tech.* 2012; **30**, 131-5.
[21] L Piancastelli, L Frizziero, S Marcoppido and E Pezzuti. Methodology to evaluate aircraft piston engine durability. *Int. J. Heat Tech.* 2012; **30**, 89-92.
[22] L Piancastelli, L Frizziero, G Zanuccoli, NE Daidzic and I Rocchi. A comparison between CFRP and 2195-FSW for aircraft structural designs. *Int. J. Heat Tech.* 2013; **31**, 17-24.
[23] L Piancastelli, L Frizziero, NE Daidzic and I Rocchi. Analysis of automotive diesel conversions with KERS for future aerospace applications. *Int. J. Heat Tech.* 2013; **31**, 143-54.
[24] L Piancastelli, L Frizziero and I Rocchi. An innovative method to speed up the finite element analysis of critical engine components. *Int. J. Heat Tech.* 2012; **30**, 127-32.
[25] L Piancastelli, L Frizziero and I Rocchi. Feasible optimum design of a turbo compound Diesel Brayton cycle for diesel-turbo-fan aircraft propulsion. *Int. J. Heat Tech.* 2012; **30**, 121-6.
[26] L Piancastelli, L Frizziero, S Marcoppido, A Donnarumma and E Pezzuti. Fuzzy control system for recovering direction after spinning. *Int. J. Heat Tech.* 2011; **29**, 87-93.
[27] L Piancastelli, L Frizziero, S Marcoppido, A Donnarumma and E Pezzuti. Active antiskid system for handling improvement in motorbikes controlled by fuzzy logic. *Int. J. Heat Tech.* 2011; **29**, 95-101.

[28] L Piancastelli, L Frizziero, E Morganti and E Pezzuti. Method for evaluating the durability of aircraft piston engines. *Walailak J. Sci. & Tech*. 2012; **9**, 425-31.
[29] L Piancastelli, L Frizziero, E Morganti and A Canaparo. Embodiment of an innovative system design in a sports car factory. *Far East J. Electron. Comm.* 2012; **9**, 69-98.
[30] L Piancastelli, L Frizziero, E Morganti and A Canaparo. The electronic stability program controlled by a fuzzy algorithm tuned for tyre burst issues. *Far East J. Electron. Comm.* 2012; **9**, 49-68.